Toughening styrene maleic anhydride copolymers with functionalized ethylene propylene rubbers

N. Dharmarajan and S. Datta
Polymers Group, Exxon Chemical Company, Linden, NJ 07036, USA
(Received 19 June 1991; revised 22 August 1991; accepted 30 August 1991)

This study describes the impact modification of brittle styrene maleic anhydride (SMA) copolymers with primary amine functionalized ethylene propylene (EP) elastomers. Compatibilization of functional EP in SMA is achieved by chemical reaction of complementary functional groups to form a graft in situ. *FT*i.r. methods and differential solvent extraction techniques demonstrate graft copolymer formation. Morphological studies indicate that the domain size of the dispersed elastomer ranges from 1 to 3 μm. This may represent an optimum for SMA, which fails by crazing. Rheological characteristics of SMA and SMA/EP blends were studied by using both capillary and parallel-plate viscometers. Graft polymer formation does not substantially increase viscosity at high strain rate, but introduces an apparent yield stress at low shear.

(Keywords: toughening; styrene maleic anhydride copolymers; ethylene propylene elastomers)

INTRODUCTION

The most important developments in the utilization of existing polymers are the rapid developments of blends, alloys and composites. These materials are important because (a) their properties can be tailored by a combination of composition and processing and (b) under favourable experimental conditions it is possible to have synergistic improvement in a property or a group of properties without the need for the development of new polymers. The structure of blends and alloys that contain only polymeric components depends on two thermodynamic and kinetic factors. First, the entropy of mixing for macromolecules is small so that most pairs of polymers are immiscible or insoluble in each other. Thus in the absence of a favourable chemical interaction ($\Delta G < 0$) between the two polymers separation of the polymers into two distinct phases is preferred. Secondly, the macromolecular chain structure of these polymers also makes the dynamics of complete disentanglement of polymers and consequent gross separation of phases slow. The combination of these factors causes most well-mixed polymer blends to have discrete phases in a size range greater than several micrometres. It is often important to obtain sizes smaller than this since the mechanical (e.g. impact strength), rheological (e.g. viscosity and yield stress) and synergistic improvements in properties depend on it. In general, control of the blend morphology provides control of properties.

One of the methods for obtaining such control is through the use of compatibilizers. These are block or graft polymers that act as interfacial agents[1-3]. These molecules preferentially reside at the interface in the blends because one segment of the compatibilizer is miscible with one component and another segment with the other. The architecture of the polymeric compatibilizers is variable, but must, at least, contain different polymer segments, chemically linked together, where each segment in turn is compatible with one of the phases in the blend system. Usually individual blocks of the compatibilizer are identical to the components of the blend. There are two effects for the presence of the compatibilizer: the adhesion between the phases increases[4] and the interfacial tension between them (ψ) decreases. At some level of the compatibilizer ψ drops to zero so that there is a finite small size (and corresponding surface area) of the domains which are in thermodynamic equilibrium. Even when ψ is not zero, the fact that it is smaller than it would be without compatibilizer indicates that a finer dispersion of the phases can be achieved during intensive mixing[5-7].

In a non-compatibilized blend the interfacial tension increases with differences in solubility parameter between the component polymers. When this difference is less than 0.5 $cal^{1/2}$ $(cm^3)^{-1/2}$ micrometre-sized morphology of the dispersed polymer phase is possible[8] by simple intensive shear mixing. This is true for blends based on chemically closely related polymers such as ethene propene copolymers (EPR) and polypropylene (PP). High shear melt mixing of EPR and PP produces fine dispersions of EP particles with domain sizes in the range 1–5 μm[9]. In our case, the difference in solubility parameter between the component polymers is large (about 1.5 $cal^{1/2}$ $(cm^3)^{-1/2}$) and simple high-intensity mixing leads to neither good interfacial adhesion nor micrometre-sized morphology. Both of these results are easily achieved in the presence of the compatibilizer. The smaller size and the increased phase adhesion leads to improvements in physical properties such as impact strength[10] and tensile strength[11].

The difficulty in synthesizing such compatibilizers is

0032-3861/92/183848-10

that experimental procedures for directly polymerizing a block polymer containing segments of EPR and SMA are unknown. EPR copolymers are usually made in a solution Ziegler polymerization procedure, while styrene maleic anhydride copolymers are usually made in a bulk free-radical polymerization. We are unaware of any polymerization procedure that would incorporate these different monomers into a single polymer chain; the question of organizing them into segments of the above composition thus does not arise. However, the compatibilizer can be chemically generated during the blending process if the polymers contain complementary, reactive functionality. Such an approach has been previously described for impact modification of polyesters and polyamides with maleic anhydride functionalized EP polymers[12]. In this paper the synthesis of a EP-*g*-SMA graft polymer is demonstrated. This is a two-step process where EP containing incorporated primary amine functionality is made first[13] and then reacted with the maleic anhydride groups of SMA to form the graft polymer, where the connecting link is the imide linkage. We prove the formation of the graft polymer by several independent methods and use it as a compatibilizer for EP/SMA blends.

The use of rubbers (e.g. polybutadiene rubber) to toughen brittle polymers (e.g. polystryene) is widespread[14]. The effect and mechanism of rubber toughening[15] have been determined to depend on both the properties of the rubber as well as the failure mode of the plastic. The effectiveness of rubber toughening depends on the weight fraction of rubber and the morphology of dispersed rubber phase[14,15]. Kim *et al.*[16] indicate that the predominant failure mode in SMA is crazing. This has been experimentally verified by the authors from post-yield volume-change measurements obtained during tensile testing. This is in contrast to the combination of yielding and crazing that dominates the failure of styrene–acrylonitrile (SAN) copolymers[17]. It is well known that the most efficient use of the elastomer in rubber-toughening brittle styrene copolymer resins requires that the rubber particle size is larger than the critical size of about 1–6 μm[14,17]. Small particles less than 1 μm in size are not effective in terminating catastrophic craze prorogation in the polymer matrix. This suggestion has not been tested experimentally in SMA resins since variation of the rubber particle size has not been demonstrated in prior studies on impact-modified SMA.

Kim *et al.*[16] used SAN grafted to butadiene rubber as the elastomer in impact-modifying the SMA matrix. SMA and SAN form a miscible polymer pair when the styrene contents of the two polymers are equivalent. This graft polymer acts as the compatibilizer and determines the morphology of the dispersed polybutadiene rubber phase. In an alternative approach, Willis *et al.*[18] have reacted bromobutyl rubber with dimethylaminoethanol (an α,ω-hydroxyamine) to form the quaternary ammonium salt of butyl rubber containing a pendant hydroxy functionality. This reacts with SMA in a subsequent blending operation to form a compatibilizer in situ. By using this approach of compatibilizer synthesis a fivefold reduction in the size of the dispersed butyl phase was observed.

In this paper the synthesis and use in compatibilization of a graft copolymer consisting of the reaction product of SMA and a random amine functionalized EP are described. SMA is a random copolymer of styrene and maleic anhydride. The incorporation of maleic anhydride as a comonomer in SMA increases its heat-distortion temperature relative to polystyrene (PS). However, SMA resins are brittle and require impact modification for engineering applications. SMA resins are available as Dylark® polymers from Arco Chemical Co. Synthesis of primary amine functionalized EP polymers have been described elsewhere[13]. The distribution of reactive, functional groups in the EP polymer is, to the best of our understanding, random along the chain. The concentration of functional groups can be controlled from zero to more than 2 mol% in our polymerization procedure, but we have used polymers that have about 0.3–0.5 mol% of functionality. For a polymer with a number average molecular weight (M_n) of 80000, this corresponds to 6–10 amine groups per chain. The characteristics of the functional EP polymer and the SMA resins are shown in *Table 1*.

EXPERIMENTAL

Blending and moulding

SMA resins and functional EP polymer at varying weight fractions were melt blended in a high-intensity shear mixer (Brabender Plasticorder®) by using a 300 g batch size and a cycle time of 4 min. The rotor speed of the mixer was adjusted so that the maximum temperature of the batch did not exceed 220°C, in order to prevent thermal degradation of the blend components. The compounds prepared in the mixer were ground into pellets.

Test specimens were prepared by injection moulding in a 20 ton Boy® machine. The nozzle temperature of the moulding machine was varied in intervals of 20°C from 190°C to 270°C. The notched izod impact strength measured at 21°C was determined at each moulding

Table 1 Polymer characteristics

Polymer	Mooney viscosity ML(1+4) 125°C	Molecular weight ($\times 10^3$)			Amine (mol%)
		M_w	M_n	M_w/M_n	
SMA-1[a] (8 wt% MA)	–	200	100	2.0	–
SMA-2[a] (14 wt% MA)	–	180	90	2.0	–
EP (56 mol% ethylene)	21	120	57	2.0	0.3

[a]From Kim *et al.*[16] MA is maleic anhydride

condition. The test bars moulded at the lower nozzle temperatures (190°C) contained a visible 'skin' layer which delaminated from the specimen. At the higher nozzle temperature (250°C) the specimens were homogeneous with no visible skin layer. The optimum impact performance was also observed from samples moulded with a nozzle temperature 250°C. This temperature was used for subsequent specimen preparations.

Testing

Mechanical properties such as room-temperature notched izod impact strength (ASTM D256, Method A), heat-distortion temperature (ASTM D 1637) at 1.8 MPa (264 psi), flexural modulus (ASTM D790, Method A) and tensile strength (ASTM D638) for these blends were obtained from injection-moulded bars 3 mm (1/8″) thick by using the ASTM methods indicated. The heat-distortion temperature (h.d.t.) measurement unit was calibrated against standard polycarbonate specimens of known h.d.t. values. The accuracy of the unit was determined to be ±3°C.

Differential scanning calorimetry

Thermal properties of the polymer blends were measured with a Dupont 9000 differential scanning calorimeter (d.s.c.). The samples were converted into thin films by applying a compressive stress at 200°C for 10 min. Upon removal from the press, the films were annealed at 21°C for 2 days before analysis. D.s.c. thermograms (first heat curve only) were obtained at a constant heating rate of 20°C min^{-1} in the temperature range from −100°C to 300°C.

FT*i.r. analysis*

*FT*i.r. spectra from pressed film samples of neat SMA and elastomer-modified SMA were obtained to identify the presence of imide and amide links formed during melt processing.

Microscopy

Morphology of the moulded samples was studied with both light microscopy and scanning electron microscopy (SEM). Samples for SEM analysis were microtomed cryogenically and stained with RuO_4. A Jeol 35C SEM was used to examine the morphology of the prepared samples. Imaging was performed with a Robinson back-scattered electron detector for enhanced clarity.

Rheology

Rheology properties were measured in a Gottefert 2001 capillary rheometer with a capillary 30 mm long and 1 mm in diameter. Viscosity measurements at varying shear rates were obtained for both unmodified SMA and blends of SMA with EP at temperatures of 250°C and 300°C. Rheological measurements at low shear rates were measured from dynamic oscillations in a Rheometrics Mechanical Spectrometer, System IV, by using a constant strain amplitude of 10%.

RESULTS AND DISCUSSION

Mechanical properties of modified SMA

Figure 1a shows the variation in notched izod impact strength at 21°C of SMA-1 (8 wt% MA) modified with EP at varying modifier levels. Unmodified SMA-1 is a brittle polymer with notched izod impact (21°C) of 27 J m^{-1}. The use of an EP modifier leads to a significant improvement in impact performance. For example, at 25 wt% modifier the impact strength is enhanced by a factor of 8 to 220 J m^{-1}. The enhancements in impact strength of SMA-1 modified with EP shown here are significantly greater when comopared to other studies on SMA modification. This comparison is included in *Figure 1a*. The approach by Kim *et al.*[16] of using SAN-grafted butadiene rubber as the modifier produces impact improvements of only a factor of four at 25 wt%

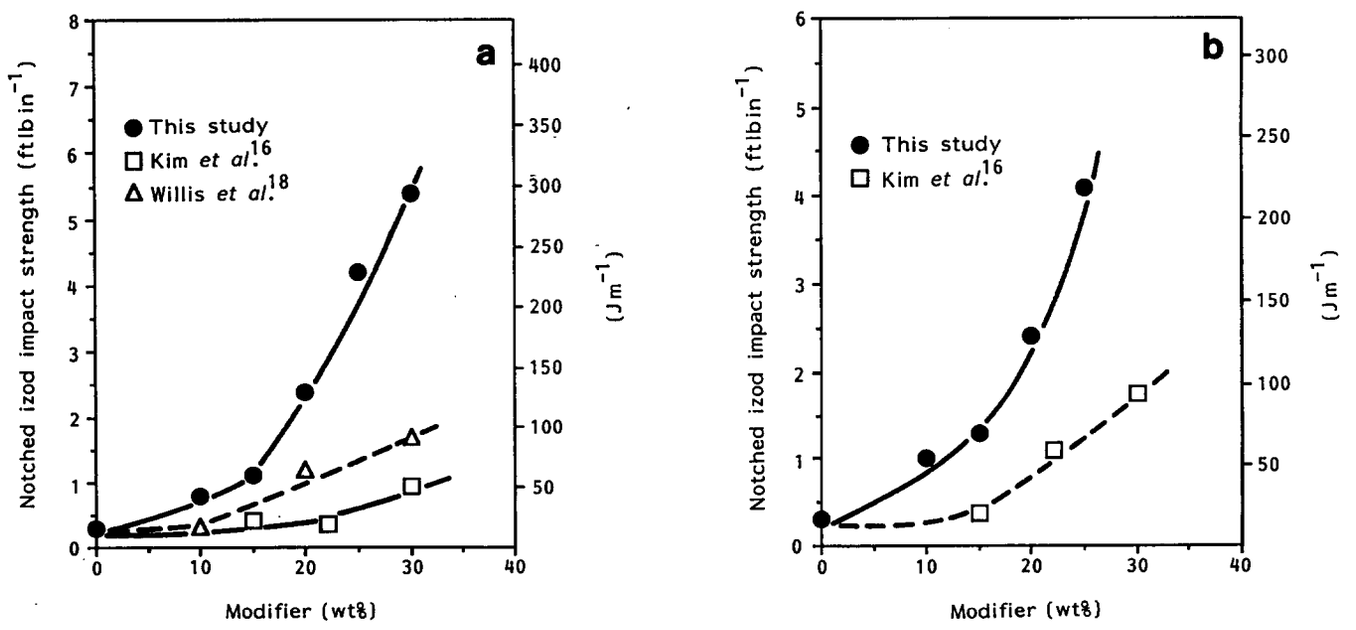

Figure 1 Influence of functional modifier levels on SMA impact properties measured at 21°C: (a) SMA-1 containing 8 wt% MA; (b) SMA-2 containing 14 wt% MA

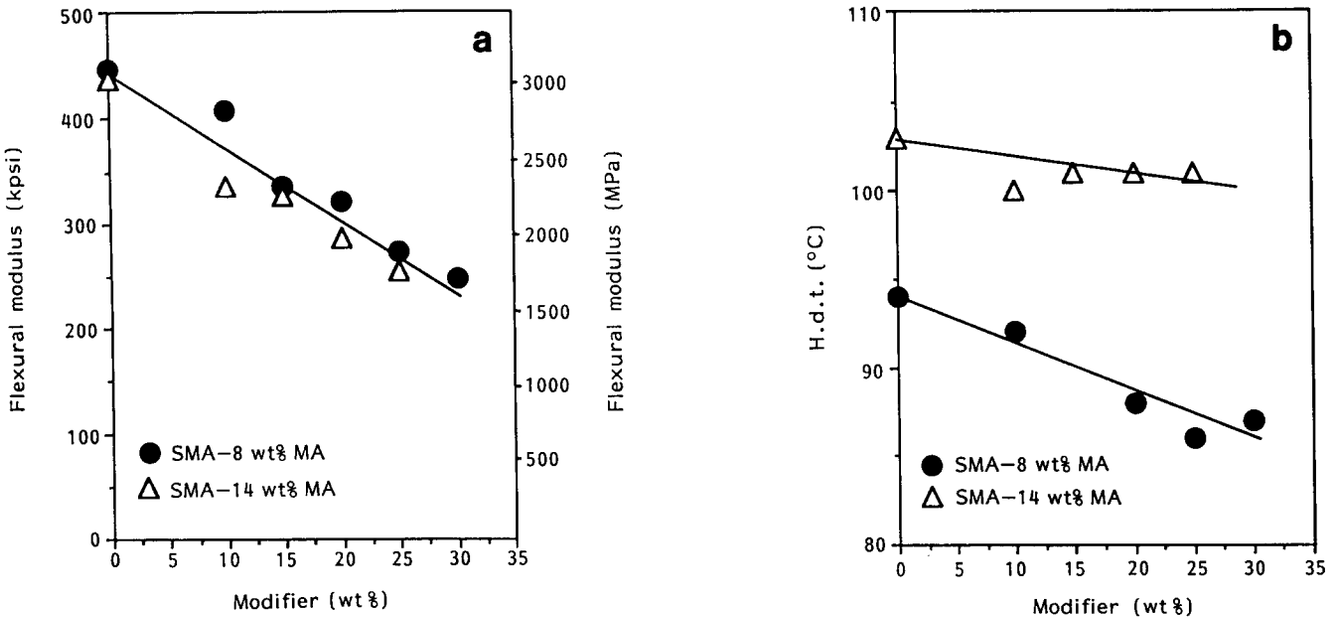

Figure 2 Mechanical properties of impact-modified SMA systems: (a) variation of flexural modulus with modifier level; (b) variation of h.d.t. at 264 psi (1.8 MPa) load with modifier level

elastomeric modifier. The use of butyl rubber with a compatibilizer as reported by Willis *et al.*[18] does not seem to produce substantial toughening of the SMA matrix. Similar toughening of SMA-2 (14 wt% MA) by EP is seen in *Figure 1b*. The use of EP modifier produces significant toughening compared to the acrylic elastomeric modifier system used by Kim *et al.*[16].

Figure 2a illustrates the change in flexural modulus with increasing EP modifier levels. *Figure 2b* shows the variation in h.d.t. with modifier content. As expected, with increasing elastomer level there is a reduction in both flexural modulus and h.d.t. With the addition of 25 wt% modifier to SMA-1, the flexural modulus drops from about 300 to 170 MPa. The h.d.t. for the same system decreases from 94°C for the unmodified SMA-1 to 88°C at 25 wt% modifier. Changes in h.d.t. for SMA-2 with modifier content appear much smaller. Our data on mechanical properties demonstrate that the EP modifiers cause acceptable reduction in stiffness and do not substantially alter the heat resistance of SMA resins; which is critical for structural applications.

The commercial importance of this work is that it provides an alternative to the current procedure of impact-modifying SMA by copolymerizing polybutadiene rubber (PBD) into SMA (Dylark® 350, Arco Chemical). These impact-modified SMA compositions are believed to be deficient in their weatherability characteristics. Weatherability is enhanced in our blends since we use a fully saturated EP backbone as the rubber modifier instead of a polyunsaturated polybutadiene rubber. *Table 2* shows the changes in mechanical properties of a SMA-1/EP blend containing 30 wt% modifier after exposure to ultraviolet light (u.v.) for 48 h at 80°C. A SAN-*g*-EPR (Rovel® 701, Dow Chemical Co.) graft polymer, which is a specified resin for outdoor applications requiring weatherability, was used as control. The SMA-1/EP blend retains its properties after u.v. exposure with no signs of discolouration and compares favourably with the SAN-*g*-EPR system.

Table 2 Changes in mechanical properties after exposure to u.v. light

System	Percentage change in property		Appearance after u.v. exposure
	Notched izod impact (21°C)	Flexural modulus	
SMA-1/EP (30 wt% modifier)	15	0	No discolouration
SAN-*g*-EPR (Rovel® 701)	−1	1	No discolouration

Compatibilization mechanism

Grafting of EP and SMA occurs by the chemical reaction illustrated in *Figure 3a*. The primary amine functionality in EP reacts with the maleic anhydride moieties in SMA to form imide linkages. The progress of this reaction can be monitored by changes in the i.r. absorbances of the blend: these are diagnostic of reaction at the maleic anhydride residues. For the blend ratios of 70/30 of SMA and EP, only 2–5% of the maleic anhydride residues are reacted. Thus the expected decrease of the maleic anhydride band at 1760 cm^{-1} is too small to be observed experimentally. However, the reaction of amine groups in EP with the anhydride groups of SMA to form imides does lead to the formation of new carbonyl groups (C=O groups in imide), which are visible as separate and distinct absorbances in the i.r. spectra. An example of such a reaction product is shown in *Figure 3b*, which shows the presence of a new carbonyl resonance at 1735 cm^{-1} from the reaction of SMA-1 and EP.

It is important to realize that despite the reaction between EP and SMA-1, both of which are multi-functional molecules, significant gel formation by cross-linking does not occur. This is shown in the bulk rheology data discussed later. This result is at variance with the classic mean-field gel-point conversion

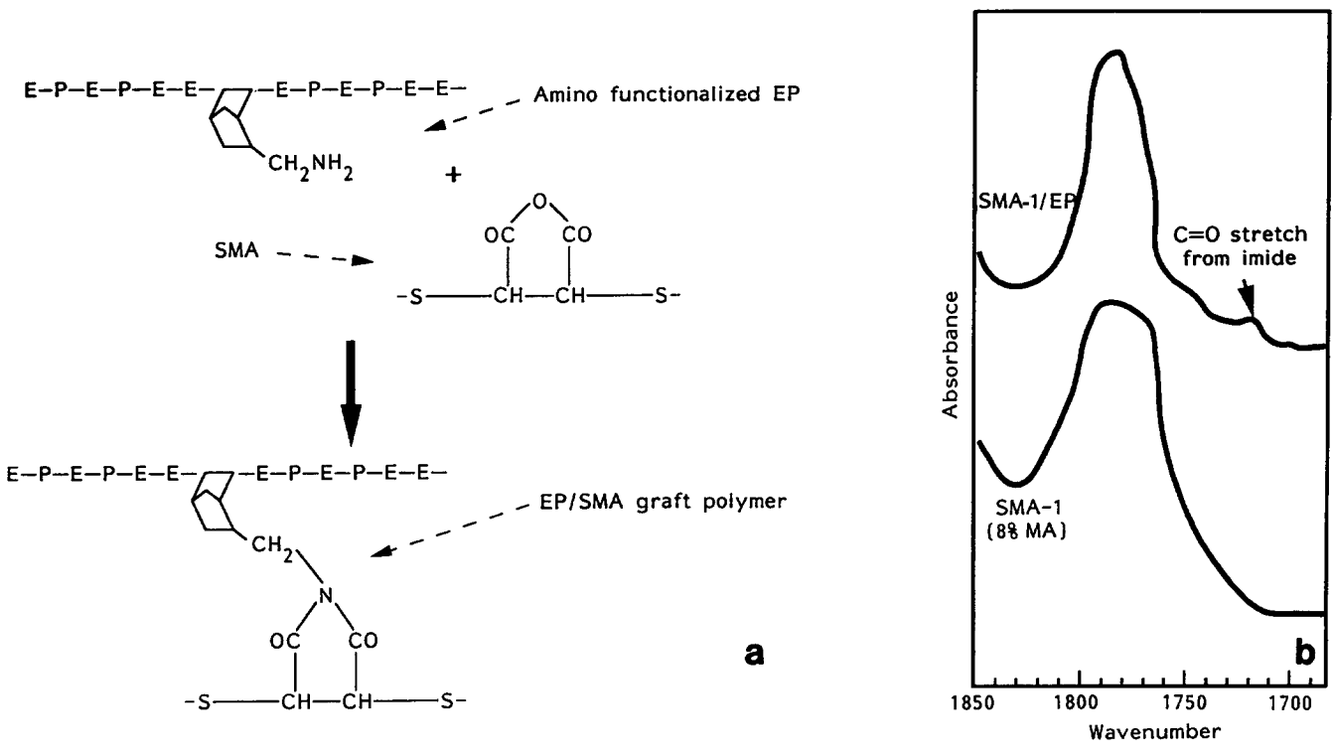

Figure 3 (a) Reaction mechanism for formation of EP-*g*-SMA (E, ethene; P, propene; S, styrene); (b) *FT*i.r. spectra of unmodified SMA-1 and SMA-1 modified with functional EP

calculation[19] with $\rho_a\rho_b(f_a - 1)(f_b - 1) = 1$, where the ρ_i are extents of reaction and f_i are the functionalities at the gel point. With 0.3 mol% NH_2 in EP, the ratio of amine to maleic anhydride for the extreme case of 30 wt% modifier is about 3.4×10^{-3}. If it is assumed that SMA-1 has 40 maleic anhydride groups per weight-average molecule ($f_a = 40$) and the functional EP has 16 amine groups ($f_b = 16$), then it is estimated that gelation should occur when ρ_a is about 0.25 and ρ_b is 8.5×10^{-4}. The fact that we do not have much gel indicates that the reaction proceeds to a lesser extent and probably only near the interface. This is plausible since coil interpenetration of EP and SMA-1, which is a necessity for these reactions, does not occur readily. These calculations are supported by differential solvent extraction data, which show only reaction of a small portion of the two phases.

Figure 4 shows d.s.c. thermograms of SMA-1 resin, EP and modified SMA-1 containing 30 wt% modifier. From the d.s.c. curves, the glass transition temperature (T_g) of the EP modifier is approximately -45°C, while for the SMA polymer it is about 125°C. The blends of SMA-1 and EP show both of the T_gs of the component polymers, which is characteristic of immiscible polymer blend systems.

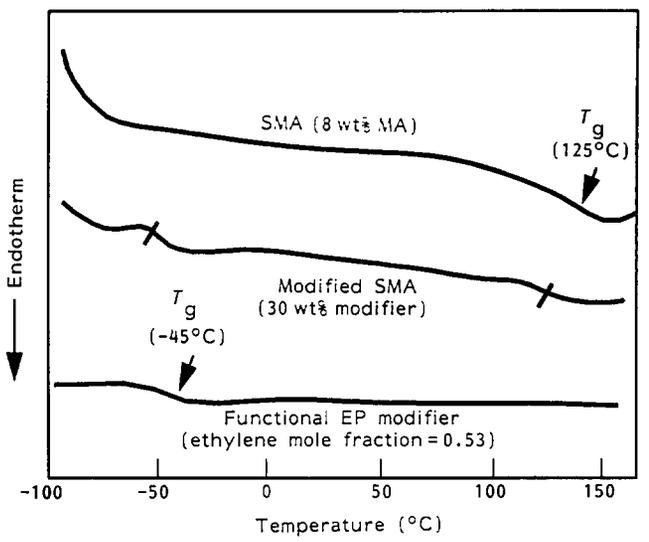

Figure 4 D.s.c. thermograms of SMA-1, functional EP modifier and modified SMA-1 at 30 wt% modifier level

Differential solvent extraction

Evidence that the chemical reaction (*Figure 3a*) does lead to the formation of a graft of SMA and EP polymer is obtained by a differential solvent extraction experiment. In this procedure a 2.5 mm thick pad consisting of the blend containing EP or EPR (EPR is a non-functionalized copolymer having 0.53 mol fraction of ethylene and a M_w (by gel permeation chromatography) of 1.4×10^5) and SMA-1 in a ratio of 50/50 by weight is successively extracted with acetone at 41°C followed by refluxing iso-octane at 94°C and finally with acetone at 41°C. Both acetone extracts are combined and treated analytically as a single fraction. SMA-1 is only soluble in acetone, while EP or EPR is only soluble in iso-octane: any gel formed during blending would be retained as insoluble material after these extractions. Control extraction experiments with a coarse (unblended) mixture of EP and SMA indicate that under the acetone extraction conditions reaction of amines and anhydrides is minimal. The two soluble fractions from each extraction and the gel, if any, are isolated and analysed by i.r. spectroscopy for (i) relative amounts of EP or EPR and SMA-1 and (ii) the extent of reaction of

Table 3 Analysis of the solvent fractionation data for SMA-1/EP blends

	Acetone fraction[a]		Iso-octane fraction[a]		Insoluble fraction[a]	
Sample[b]	SMA-1	EP*	SMA-1	EP*	SMA-1	EP*
EP* = EPR	0.49	0.01	0.01	0.49	–	–
EP* = EP	0.45	0.03	0.04	0.45	0.01	0.03

[a]Composition of the fractions are expressed as the weight fraction of the total weight of the blend
[b]All samples contain 50 wt% SMA

amines and anhydrides. Absorption bands at 722 cm^{-1} and 1012 cm^{-1}, which are identifiable with EP and SMA-1, respectively, have been used for the first analysis, while the relative intensities of the carbonyl bands arising from anhydride (1760 cm^{-1}) and imide (1735 cm^{-1}) functionalities are used for the second analysis.

Blends of SMA-1 and EPR are 'cleanly' separated in this fractionation procedure. This is shown by the data in *Table 3* (sample EP* = EPR), where the fractionation of this blend of non-reactive pair of polymers leads to an acetone-soluble fraction, which is all the SMA-1 in the blend, and an iso-octane-soluble fraction, which is all of the EPR in the blend. The significant results are (i) the absence of contamination of either the EPR or the SMA-1 fraction by SMA-1 or EPR, respectively, and (ii) absence of conversion of anhydride in SMA-1 to imide functionality. The situation is significantly different for the reactive blends of functionalized EP and SMA-1. The data in *Table 3* (sample EP* = EP) show that (i) the acetone-soluble fraction contains 90% of the total amount of SMA-1 present in the blend and 8% of the EP, (ii) the iso-octane fraction contains 90% of the EP and 8% of the SMA in the blend and (iii) the insoluble gel contains the remaining 1% of the SMA-1 and 3% of the EP. Analysis of each of the above fractions indicates (i) that the acetone-soluble fraction does not appear to have any imide and (ii) that the gel fraction has almost all of the available amine groups on the EP converted to the imide by reaction with SMA-1. Most of the blend material is isolated in either the acetone or the iso-octane fraction with comparatively little appearing as the grafted gel. The composition of all of the fractions is neither pure EP nor SMA-1, but rather a mixture of the two. The degree of cross-contamination of the phases is a measure of the extent of the grafting reaction between the SMA-1 and EP backbone. The amount of graft polymer formed is comparatively small and it is estimated that less than 10% of either of the two phases is involved in this reaction.

Morphology

These graft polymers are active as compatibilizers in the EP/SMA blend system. This is most easily studied in 70/30 blends of SMA and EP because of the ease in microscopic determination of morphology. Visual inspection of the fracture surface showed signs of stress-whitening, which is typical of rubber-toughened plastics. Samples for morphology were initially examined under a light microscope as thin sections (50–100 nm) by using phase contrast. The light phase in the micrographs represent the EP modifier *Figure 5* shows the differences in particle size of the dispersed elastomer phase for the SMA-1/EP systems containing (a) a non-functional EPR and (b) a functional EP modifier. The blend containing non-functional EPR shows no compatibilization, as shown by the large particles that are typically produced by mixing of high-viscosity components with high interfacial energy[14]. The elastomer domains are elliptically distorted in the direction of the injector flow with the minor axis being about 5–8 μm, while the major axis is about 20–40 μm. There is also no improvement in impact performance over unmodified SMA resins. In contrast, blends of functional EP in SMA (*Figure 5b*) show a very fine morphology where the EP domains are approximately spherical with a diameter of about 1–3 μm. *Figure 6* shows an SEM micrograph of SMA-1 resin modified with functional EP at 25 wt% modifier level. The zone size of the dispersed elastomer is about 1 μm. Both Kim *et al.*[16] and Willis *et al.*[18] have shown similar domain size of the dispersed elastomer in SMA matrix. Kim concluded that the use of a SAN-grafted polybutadiene rubber, where the grafted SAN chains are miscible with the SMA-1 matrix, produces only moderate improvements in the notched izod impact values (e.g. 100 J m^{-1} at 30 wt% elastomer content). The formation of covalent linkages betweer

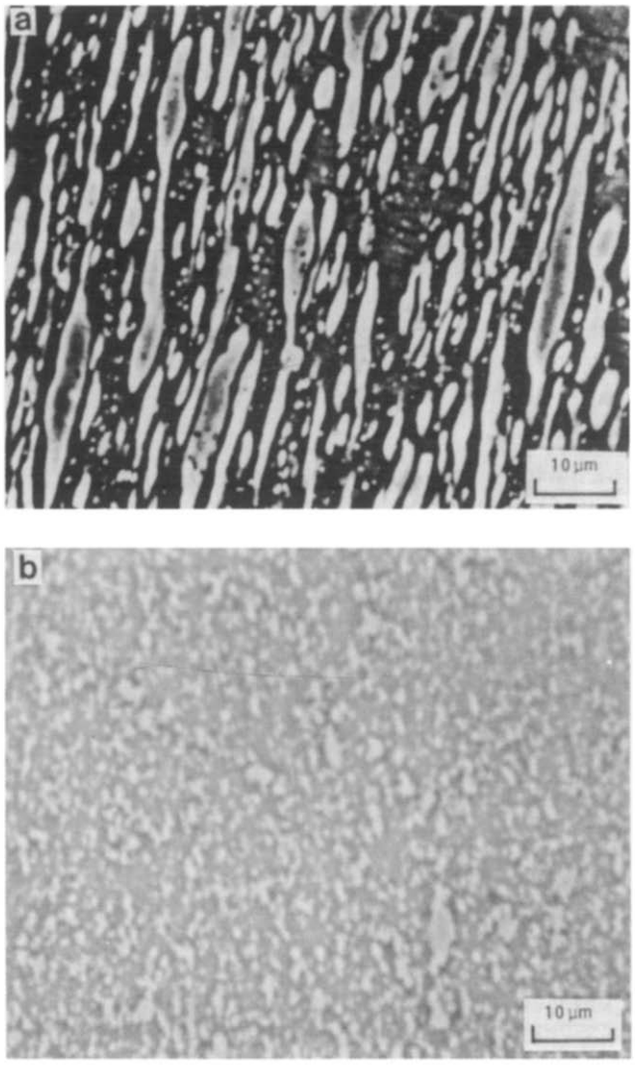

Figure 5 Light microscopy images of elastomer-modified SMA at 30 wt% modifier: (a) SMA-1 containing non-functional EPR; (b) SMA-1 containing functional EP

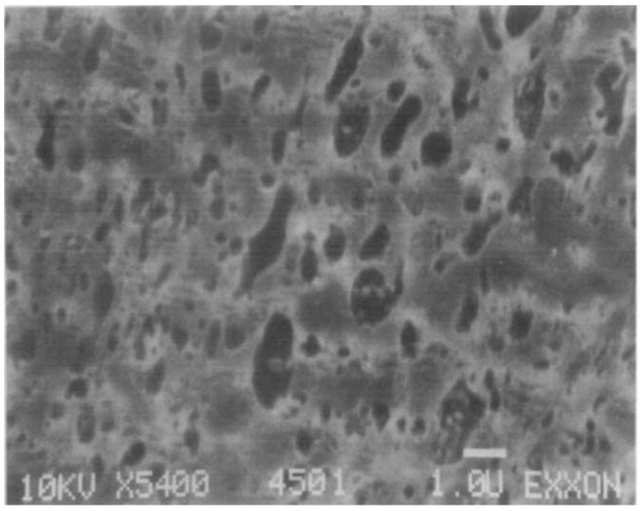

Figure 6 Scanning electron micrograph of EP modifier in SMA-1 at 25 wt% elastomer concentration

butyl elastomer and SMA-1 matrix by using a hydroxyamine connecting group, as illustrated by Willis *et al.*[18], produces elastomer particle sizes in the range from 0.5 to 1 μm at 5% hydroxyamine concentration. At this level of hydroxyamine the notched izod impact values are optimized at 90 J m^{-1} for 30 wt% elastomeric modifier. In comparison, the SMA-1/EP blend at 30 wt% modifier yields notched izod impact values of 300 J m^{-1}. Despite similar particle size distributions the toughening enhancements of SMA-1 matrix are significantly different between our work and previous studies. It is likely that other factors such as interfacial adhesion, which are more difficult to quantify, significantly influence the toughening characteristics.

The optimum rubber-particle size required for effective toughness enhancements depends on the failure mode of the matrix resin. Recently, Wu[20] has shown that the chain-entanglement density (v_e) of the matrix polymer defines the failure mode. Polymer matrices with a low chain-entanglement density (<0.15 mmol cm^{-3}) are brittle and fail by craze formation, while polymer systems with a higher entanglement density (>0.15 mmol cm^{-3}) are pseudo-ductile and tend to yield rather than craze.

The entanglement density is calculated from:

$$v_e = \rho_a / M_e \quad (1)$$

where M_e is the molecular weight of an entanglement strand and ρ_a is the amorphous mass density of the matrix resin. M_e is further determined from the relation

$$M_e = \rho RT / G_N \quad (2)$$

in which ρ is the melt density of the polymer at a temperature T, R is the gas constant and G_N is the plateau modulus. In brittle polymer systems such as polystyrene ($v_e = 0.056$ mmol cm^{-3}) and styrene maleic anhydride resins ($v_e = 0.038$ mmol cm^{-3}), the predominant failure mechanism is crazing rather than shear yielding. Such systems are optimally toughened by large rubber particles. Studies on high-impact polystyrene[21] have confirmed that particles in the domain-size range of 1–6 μm are most effective in matrix toughening. Small rubber particles of less than 1 μm are not effective in terminating catastrophic craze propagation and consequently do not significantly improve impact performance. For polymer systems that are more ductile (e.g. polyvinylchloride (PVC), $v_e = 0.252$ mmol cm^{-3}), where the failure mechanism is probably a combination of crazing and shear yielding, it is less important to have large rubber particles. These systems are best toughened by smaller particles (<1 μm), which are more effective in initiating yielding. Chain entanglement density for SMA-2 was calculated by using equations (1) and (2). *Figure 7* shows a plot illustrating the inverse relationship of optimum rubber-particle size with calculated chain-entanglement density for brittle polymer systems described by Wu[20]. The particle size range of the amine EP used in modifying SMA-2 matrix is also shown in the same figure and falls on the plot. It is believed that this particle size may be optimal, based on investigations of other polystyrenic systems that fail by crazing[20,21].

Rheology studies

Rheological properties of elastomer-modified SMA are important for polymer processing. Based on the application, the processing methods could involve injection moulding (shear rates exceeding 10^3 s^{-1}), extrusion (shear rate about 10^2 s^{-1}) or blow moulding (shear rates <10 s^{-1}). In this work the range from 10^4 to 10^{-2} s^{-1} was studied by employing capillary and parallel-plate oscillating rheometers. In the SMA/EP blends it was felt that the formation of graft polymer might cause a significant rise in the viscosity. *Figure 8* shows the measured viscosity at 250°C for varying shear rates (γ) for neat SMA-1 and SMA-1/EP blends containing 25 wt% functional EP. The standard error in measurement was about 20%. There is good agreement in viscosity measurements obtained by using the two different test methods at this precision. *Figure 9* contains the corresponding elastic modulus data obtained by using a parallel-plate viscometer for the systems shown in *Figure 8*. SMA-1 behaves like a non-Newtonian viscoelastic fluid with a constant viscosity at zero shear

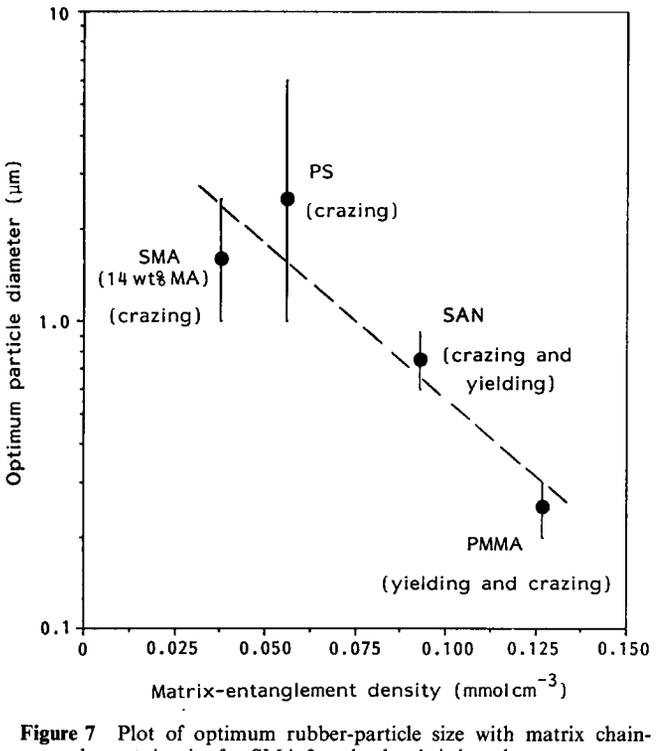

Figure 7 Plot of optimum rubber-particle size with matrix chain-entanglement density for SMA-2 and other brittle polymers

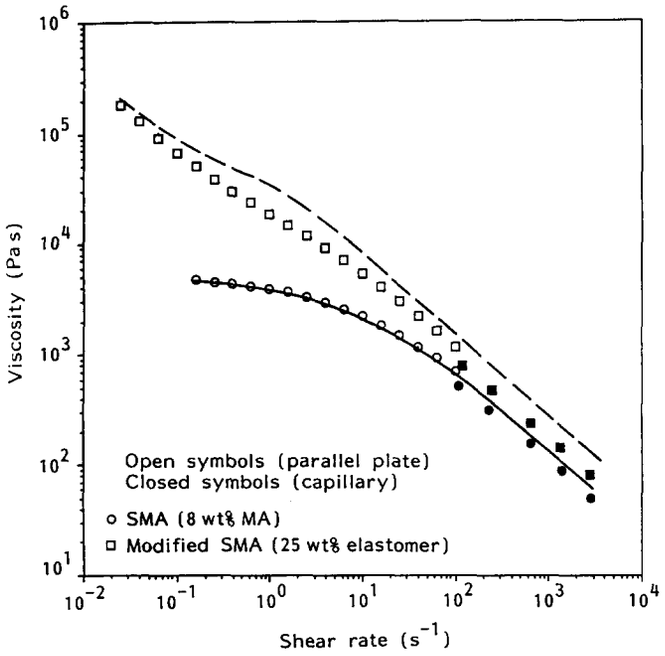

Figure 8 Rheological characteristics of SMA-1 resin and elastomer-modified SMA-1 at 250°C obtained from both capillary and parallel-plate viscometers: broken line, equation (9); solid line, equation (8)

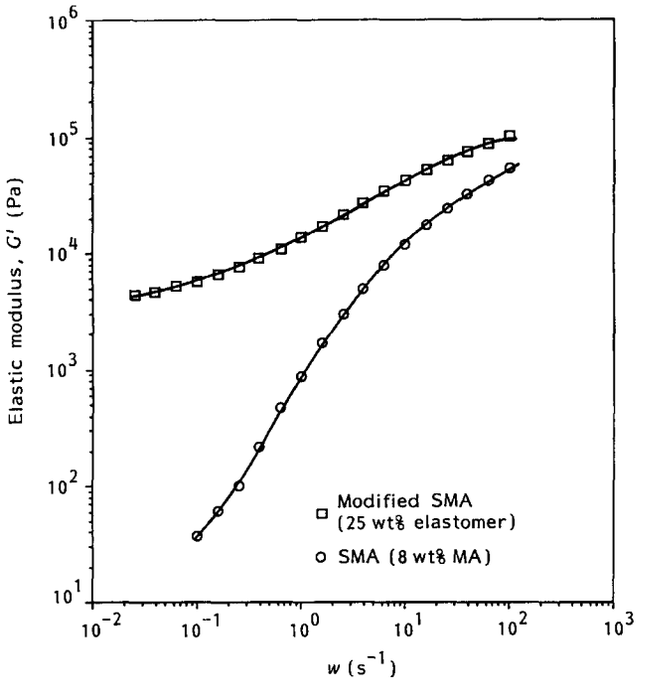

Figure 9 Variation of elastic modulus with shear rate for SMA-1 and modified SMA-1 at 250°C obtained from parallel-plate viscometer measurements (strain amplitude = 0.1)

rate, and the elastic modulus (G') decreasing to zero with a γ^2 dependence at low strain rates. In the rubber-modified system both viscosity and elastic modulus are higher than those of unmodified SMA-1, at a given shear rate, indicating that rubber incorporation enhances the capacity of the material to store elastic energy as well as to dissipate mechanical energy. At low shear rates the complex viscosity (η^*) increases unbounded and the elastic modulus approaches a constant value. This phenomenon indicates the presence of a yield stress.

In polymer melts that possess a yield stress, the total stress (σ) can be expressed as the sum of the yield stress (σ_y) and the actual stress (σ_m) governing the flow of the melt[22]:

$$\sigma = \sigma_y + \sigma_m \tag{3}$$

The corresponding expression for viscosity ($\eta = \sigma/\gamma$) becomes

$$\eta = \sigma_y/\gamma + \sigma_m/\gamma \tag{4}$$

At low shear rates the yield stress dominates ($\sigma_y \gg \sigma_m$) and equation (4) is approximated as

$$\eta = \sigma_y/\gamma \tag{5}$$

which can be further rewritten in the form

$$\log(\eta) = \log(\sigma_y) - \log(\gamma) \tag{6}$$

$$\frac{d\log(\eta)}{d\log(\gamma)} = -1 \tag{7}$$

A criterion for yield stress from equation (7) requires that a double logarithmic plot of viscosity (η) with shear rate (γ) should have a distinct slope of -1. The data in *Figure 8* for the elastomer-modified SMA-1 system indicate that for shear rates less than $3 \times 10^{-1}\ s^{-1}$, the slope of this curve is indeed -1, confirming presence of a yield stress.

There are several methods used in calculating the yield stress of polymer melts. The Casson plot[23] is a common technique. According to this method a linear plot of $(\gamma)^{1/2}$ with $(\sigma)^{1/2}$ will extrapolate to the square root of the yield stress at zero shear rate. *Figure 10* shows the Casson plot for both SMA-1 and the elastomer-modified SMA-1 system. All the experimental data points fall on the

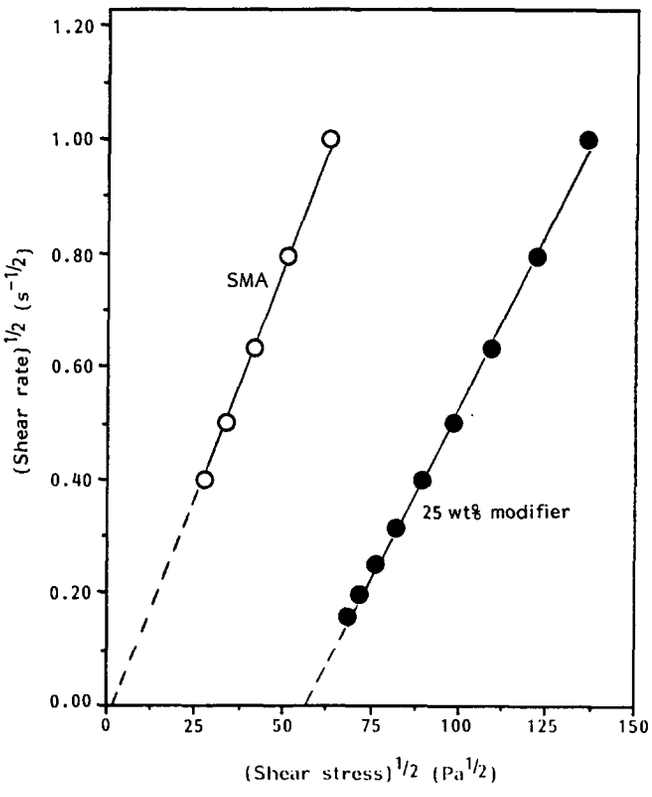

Figure 10 Casson plots of unmodified SMA-1 and elastomer-modified blend

Casson plot. The SMA-1 polymer has virtually no yield stress, while the elastomer-modified blend (25 wt% modifier) has a yield stress value of 3164 Pa.

The rheological measurements help to describe mathematically the pseudo-plastic behaviour of the polymer melts over a wide range of shear rates. The melt behaviour of unmodified SMA-1 can be adequately represented by using the equations of Elbirili *et al.*[24] and Utracki[25]:

$$\eta/\eta_0 = 1/[(1 + \tau\gamma)^{m_1}]^{-m_2} \quad (8)$$

where τ is the relaxation time and the other terms are material constants. The term η_0 is the zero shear rate viscosity. In *Figure 8*, equation (8) (solid line) is compared with the data for neat SMA-1. There is good agreement of the model with the experimental data. For polymer melts that have a yield stress, equation (8) is modified to include a yield stress term[26] in the form:

$$\frac{\eta}{\eta_0} = \frac{1}{[(1 + \tau\gamma)^{m_1}]^{-m_2}} + \frac{\sigma_y(1 - e^{-a\gamma})^u}{\gamma\eta_0} \quad (9)$$

In the limit of no yield stress ($\sigma_y = 0$), equation (9) reduces to equation (8). This model has been used previously to describe the melt behaviour of cross-linked polystyrene spheres suspended in polystyrene solutions[27].

Table 4 Material constants used in describing polymer melt rheology of SMA and modified SMA systems

System	η_0 (Pa s)	τ (s)	m_2	σ_y (Pa)	a (s)
SMA-1 (8 wt% MA)	4641	0.30	0.62	–	–
SMA-1/EP (25 wt% modifier)	101 691	97.1	0.55	3164	10000

$m_1 = 1$ and $u = 1$ for both systems
Temperature = 250°C

The model predictions of equation (9) are compared with the actual data (broken line) in *Figure 8* for the elastomer-modified SMA-1. There is reasonable agreement between the model and the data points, especially at low shear rates. The constants of equation (8) and equation (9) are summarized in *Table 4*.

Yielding in elastomer-filled systems can be conceptually associated with agglomeration of the elastomer particles[22]. This is especially true at high elastomer concentrations, where we have noticed from microscopy the presence of a co-continuous network structure of elastomer particles and SMA resin. It is realistic to assume that at low shear rates, the steady-state shear stress applied to the polymer melt is not sufficiently high to break this network structure. However, with increasing shear stress the particle agglomeration is easily removed, causing flow of polymer melt. The parameter a in equation (9) can be visualized as a characteristic relaxation time associated with this network formation. In the same equation, τ is the relaxation time for the flow of polymer melt. It is of interest to note that a is 100 times larger than τ. In addition, τ for the modified SMA is 300 times larger than the corresponding value for the unmodified SMA polymer.

Since the major application for rubber-toughened SMA involves injection moulding, our rheological studies have focused more on studying the melt viscosity at high shear rates ($>10^2\ s^{-1}$). *Figure 11a* shows the viscosity measurements made by using a capillary rheometer at two different temperatures for unmodified and elastomer-modified SMA-1. The customary Weissenberg–Rabinowitsch correction has been applied to the viscosity measurements. Bagley-type corrections were neglected in view of the relative long L/D (30/1) of the capillary. At high shear rates both equation (8) and equation (9) reduce to the form

$$\eta = \eta_0(\tau\gamma)^{m_1 m_2} \quad (10)$$

which is essentially a form of the classical power-law

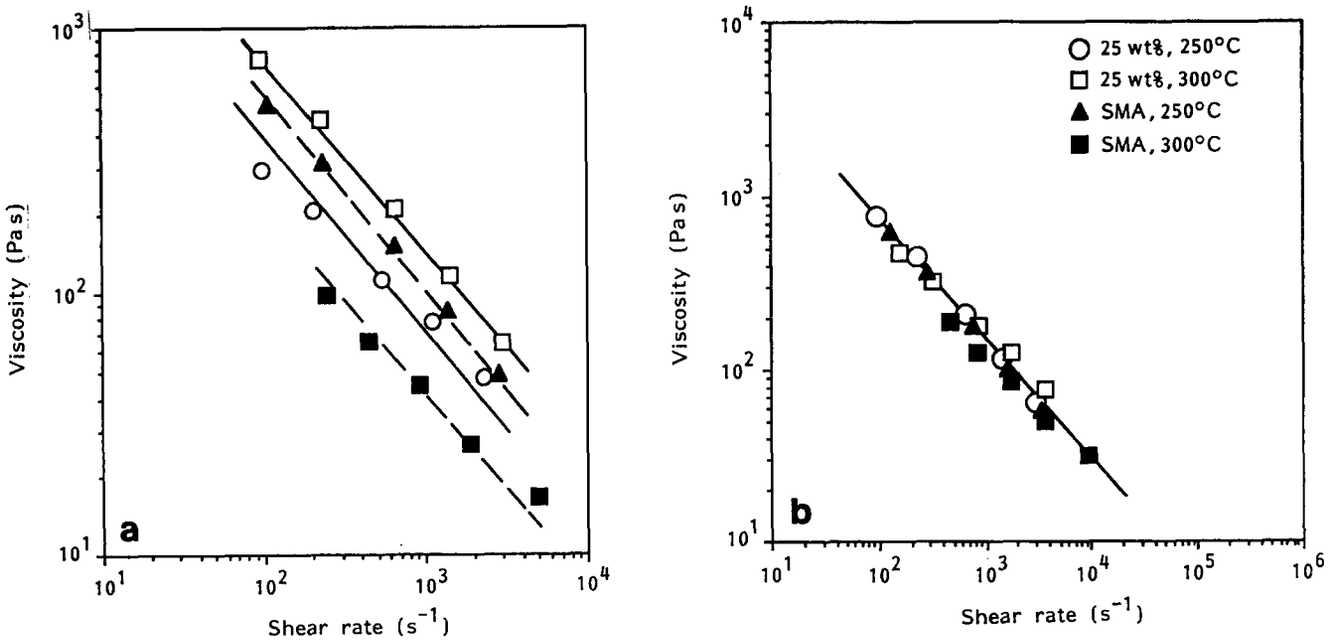

Figure 11 Capillary viscometer measurements for SMA-1 and elastomer-modified SMA-1 at varying temperatures ($L/D = 30/1$); (b) master curve of viscosity with shear rate for elastomer-modified SMA-1 (reference state chosen to be 25 wt% modifier with a temperature of 250°C)

model[28]. The exponent n ($n = 1 - m_1 m_2$) is defined as the power-law index. A value of $n < 1$ implies that the fluid is pseudoplastic or 'shear thinning'. In the limit of $n = 1$ there is no shear-rate dependence and the melt is Newtonian. Both SMA-1 and rubber-modified SMA show pseudoplastic behaviour at high shear. Interestingly the power-law exponent does not depend on the elastomer concentration. This facilitates data reduction to a single master curve of viscosity *versus* shear rate for a particular temperature at a reference modifier level. *Figure 11b* shows a master curve constructed by using the data in *Figure 11a* for the rubber-toughened SMA-1 system. The reference state was chosen to be 25 wt% modifier with a temperature of 250°C.

CONCLUSIONS

In conclusion, it has been demonstrated for the first time that EP-*g*-SMA polymers can be synthesized by reaction of SMA with directly polymerized reactive functionality on EP. The synthetic approach is novel. Blends of SMA and functional EP are toughened, presumably due to the resultant fine dispersion of the rubber in the SMA matrix and the degree of interfacial adhesion. The impact-strength improvements that have been noted here for these blends are better than those reported in previous studies. The particle size of the dispersed rubber phase in SMA for the best impact performance is about 1–3 μm: little evidence was found to support a larger optimum rubber-particle size. Smaller particles have yet to be studied.

The viscosity of modified SMA increases with increasing modifier level. However, in the SMA-1/EP blends used in this work that are 10–30% functional EP, no evidence for either extremely high viscosities or gel formation was seen. At low shear rates the rubber-toughened SMA systems show yielding, while the neat SMA has a finite zero-shear viscosity.

ACKNOWLEDGEMENTS

We are grateful to Dr F. W. Pasterczyk, Dr J. J. O'Malley and to the management of Exxon Chemical Company for their permission to publish this paper. We are particularly grateful to Dr G. Ver Strate and Dr E. N. Kresge for many insightful discussions; Dr L. G. Kaufman and Mr S. Wafalosky for their constant support and encouragement during the course of this study. We would also like to acknowledge the contributions of Ms K. Campo and Mr L. Ban for microscopy; Dr M. Monahan, Dr K. F. Wissbrun and Mr W. R. Gerald for their assistance in rheology; Dr D. M. Cheng and Mr C. B. Fredrick for *FT*i.r. analysis; and Mr W. D. Gallagher for d.s.c. measurements.

REFERENCES

1 Maglio, G. and Palumbo, R. 'Polymer Blends' (Eds M. Kryszewski, A. Galeski and E. Martucselli), Plenum, New York, 1982
2 Fayt, R., Jerome, R. and Teyssie, P. *Makromol. Chem.* 1986, **187**, 837
3 Noolandi, J. and Hong, K. M. *Macromolecules* 1984, **17**, 1531
4 Brown, H. R., Deline, V. R. and Green, P. F. *Nature* 1989, **341**, 221
5 Grace, H. P. *Chem. Eng. Commun.* 1982, **14**, 225
6 Elmendorp, J. J. and van der Vegt, A. K. *Polym. Eng. Sci.* 1986, **26**, 1332
7 Wu, S. *Polym. Eng. Sci.* 1987, **27**, 335
8 Coran, A. Y. 'Handbook of Elastomers' (Eds A. K. Bhowmick and H. L. Stevens), Marcel Dekker, New York, 1988, ch. 8
9 Kresge, E. N. *J. Appl. Polym. Sci., Appl. Polym. Symp.* 1984, **39**, 37
10 Wu, S. *Polymer* 1985, **26**, 1855
11 Coran, A. Y. and Patel, R. *Rubber. Chem. Technol.* 1983, **56**, 1019
12 U.S. Patent 4,174,358
13 Datta, S. 'High Performance Polymers' (Ed. A. Fawcett), Royal Society of Chemistry, London, 1990, ch. 2; U.S. Patent 4,987,200 (issued 11 February 1991)
14 Bucknall, C. B. 'Toughened Plastics', Applied Science, London, 1977; Newman, S. 'Polymer Blends' (Eds D. R. Paul and S. Newman), Academic Press, London, 1978, vol. 2, ch. 13
15 Donald, A. M. and Kramer, E. J. *J. Appl. Polym. Sci.* 1982, **27**, 3729
16 Kim, J. H., Keskkula, H. and Paul, D. R. *J. Appl. Polym. Sci.* 1990, **40**, 183
17 Keskkula, H., Paul, D. R., McCreedy, K. M. and Henton, D. E. *Polymer* 1987, **28**, 2063; U.S. Patent 4,366,289
18 Willis, J. M., Favis, B. D. and Lunt, L. *Polym. Eng. Sci.* 1990, **30**, 1073
19 Stockmayer, W. H. *J. Polym. Sci.* 1953, **11**, 424
20 Wu, S. *Polym. Eng. Sci.* 1990, **30**, 753
21 Keskkula, H. 'Rubber Toughened Plastics' (Ed. K. C. Riew), ACS Adv. Chem. Ser. No. 222, American Chemical Society, Washington, DC, 1989, pp. 289–290
22 Munstedt, H. *Polym. Eng. Sci.* 1981, **21**, 259
23 Casson, N. 'Rheology of Disperse Systems', Pergamon Press, New York, 1959
24 Elbirili, B. and Shaw, M. T. *J. Rheology* 1978, **22**, 561
25 Utracki, L. A. *Rubber Chem. Technol.* 1984, **57**, 507
26 Utracki, L. A. 'Polymer Alloys and Blends, Thermodynamics and Rheology', Hanser, New York, 1989, pp. 137–138
27 Onogi, S. and Matsumoto, T. *Polym. Eng. Rev.* 1981, **1**, 45
28 Cross, M. M. *J. Colloid Sci.* 1965, **20**, 417